Structures 6 (2016) 30–36

Contents lists available at ScienceDirect

Structures

journal homepage: www.elsevier.com/locate/structures

Analytical Modeling in Deformation Analysis of Interference-Fit Structures

Nelli Aleksandrova *

Faculty of Exact Sciences and Engineering, Madeira University, 9020-105 Funchal, Madeira, Portugal

ARTICLE INFO

Article history:
Received 17 July 2015
Received in revised form 15 January 2016
Accepted 17 January 2016
Available online 27 January 2016

Keywords:
Double-shear bolted joints
Strain analysis
Decohesive carrying capacity

ABSTRACT

Local analysis of bearing stresses and initiation of failure at fastener-hole location in interference-fit structures is crucial for achieving their optimal structural design and reliable service conditions. To this end, analytical research devoted to strain analysis of double-shear riveted or bolted joints is performed. The decohesive carrying capacity criterion based on the radial strains is applied and discussed. The material of the plate is considered to be elastic-perfectly-plastic obeying the Huber–Mises–Hencky yield criterion while the bolt is considered to be elastic. Due to the singularities in the radial strains and displacement at the fastener/plate interface, the problems solved analytically are of great importance for implementation of commercial numerical codes.

1. Introduction

In preliminary engineering design of compound structures such as double-shear riveted/bolted joints or pressurized containers, the modeling of cold expansion and shrink-fit processes is of great importance. The modeling of cold expansion process is usually made either with a removable or with a stay-in mandrel. The assumptions of plane-stress, the Huber–Mises–Hencky (HMH) yield criterion and elastic-perfectly-plastic or specifically hardening materials are preferred. Most of the papers devoted to compound structures consider a removable (rigid) mandrel to describe residual stress field near the fastener-hole location [1–6]. On the other hand, a stay-in mandrel is also used to describe bolted structures with an elastic bolt or insert [7,8]. The modeling of shrink-fit process as a means of solving structural engineering applications was comprehensively developed by Gamer and his co-workers on the basis of the Tresca yield criterion [9–13] influenced by the earlier works of Lundberg [14] with the HMH yield criterion and Kollmann [15] with the Tresca yield criterion. Following these theoretical studies, some combined technological processes have been successfully modeled and solved such as a) interference-fit of two circular tubes executed by cold expansion technique with or without clearance between fitting parts. This type of modeling presumes completely plastic inner part (insert) while the outer part (plate) may be elastic, elasto-plastic, or fully plastic. It was possible to get analytical solutions to this problem by employing the Tresca yield criterion and elastic-perfectly-plastic material [16,17]. b) Cold expansion of a hole with subsequent application of internal pressure or remote load [18]. c) Shrink-fit with subsequent application of internal or external pressure for fitting parts made of different materials. This problem was amenable to analytical solution due to the HMH yield criterion and assumption of plane-strain state [19]. d) Shrink-fit followed by cold expansion process [20].

Meanwhile, for analytical procedures developed to assess compound structures, the HMH yield criterion is preferred, particularly, when the elastic-perfectly-plastic material is involved. It was specifically outlined by Gamer [11] that in this case for some working pressures the Tresca yield criterion leads to a discontinuous stress field near the hole of the plate and discontinuous displacement field at the insert/plate interface.

Analytical solutions based on the HMH yield criterion all have their origin in the work of Nadai [21] who obtained distribution of stresses in an infinite plate with a circular hole subjected to uniform radial pressure. The material of the plate was assumed to be incompressible elastic-perfectly-plastic. This assumption together with a parametrization of the yield criterion permitted to derive a simple, elegant closed-form stress solution. Later on, this parametrization technique was used by Budiansky [22] who proposed a modified Ramberg–Osgood law to solve analytically the problem of orthotropic in thickness direction plate. Budiansky's procedure was successfully adopted both for infinite [1] and finite [2] plate models to obtain residual stress fields based on elastic unloading. The more advanced analysis of residual stresses with reverse yielded zones belongs to Ball [8] and Zhang et al. [23] for an infinite and finite annular plate, respectively. However, only the stress-displacement solutions were covered in both studies. As concerning elastic-perfectly-plastic material, reverse yielded zones were considered in [6], and, within elastic unloading assumption, various engineering stress solutions were presented by Aleksandrova [24] to discuss specific applications to bolted structures and pressurized

* Tel.: +351 291 705 285.
E-mail address: nelli@staff.uma.pt.

http://dx.doi.org/10.1016/j.istruc.2016.01.003
2352-0124/

containers. The comparison of various analytical models in terms of their abilities to predict residual stresses is given in [23,25–26].

As it follows from the above, analytical works on thin compound structures have been mostly devoted to residual stress analysis rather than the determination of the strain field. This justifies such assumptions as incompressible material both in the elastic and plastic zones of the plate or neglect of elastic strains in the plastic zone. However, the knowledge of the strain field is important both from the academic and engineering points of view. From the academic point of view, its importance is in the validation of the stress solution, that is, the complete stress–strain field must be continuous (not only the stress field). This is a particular concern for an elastic-perfectly-plastic material [11,27–28]. From the engineering point of view, strain analysis is important for final structural design and selection of a reliable failure criterion. However, at the moment, there is a lack of analytical research specifically devoted to the strain analysis of interference-fit structures leading to formulation of a reliable failure criterion. So, the objective of this study is to conduct such research as an extension of the earlier work on stresses [24].

2. Stress distributions in fastener-hole structures

The detailed discussion of stresses has been done in previous work [24], so, here, only necessary formulae for further kinematic analysis will be retrieved for convenience. In cylindrical coordinate system $r\theta z$ with non-zero radial, $\hat{\sigma}_{rr}$, and circumferential, $\hat{\sigma}_{\theta\theta}$, stress tensor components, consider a thin annular plate of inner radius a and outer radius b subjected to gradually increasing radial pressure $\hat{p}$ around its inner edge, $r=a$ (Fig. 1). The following boundary conditions should be satisfied:

$$\hat{\sigma}_{rr} = -\hat{p} \text{ at } r = a \text{ and } \hat{\sigma}_{rr} = 0 \text{ at } r = b \tag{1}$$

For sufficiently small values of pressure $\hat{p}$, the plate is entirely elastic. The elastic carrying capacity (when the plate just starts yielding due to the HMH yield criterion) corresponds to

$$\hat{p}/Y = \left(1-(a/b)^2\right)/\sqrt{3+(a/b)^2} \tag{2}$$

where Y is the yield stress of the plate material in tension test. For higher loads, the plate in general consists of two zones – inner plastic and outer elastic – divided by an elastic/plastic boundary, c. In the elastic zone, the material obeys the Hooke's law with the following stress–strain-displacement relations:

$$\hat{\varepsilon}_{rr} = \partial\hat{u}/\partial r = \left(\hat{\sigma}_{rr}-\nu\hat{\sigma}_{\theta\theta}\right)/E; \quad \hat{\varepsilon}_{\theta\theta} = \hat{u}/r = \left(\hat{\sigma}_{\theta\theta}-\nu\hat{\sigma}_{rr}\right)/E \tag{3}$$

where $\hat{\varepsilon}_{rr}$ and $\hat{\varepsilon}_{\theta\theta}$ are the radial and circumferential strains, respectively; $\hat{u}$ is the radial displacement; E is the Young modulus, and ν is the Poisson coefficient. In the plastic zone, the HMH yield criterion is adopted. For plane-stress state and at the absence of in-plane shear stresses, it simplifies to

$$\hat{\sigma}_{rr}^2 + \hat{\sigma}_{\theta\theta}^2 - \hat{\sigma}_{rr}\hat{\sigma}_{\theta\theta} = Y^2 \tag{4}$$

and is automatically satisfied by the standard parametric substitution

$$\hat{\sigma}_{rr}/Y = \left(2/\sqrt{3}\right)\cos\varphi, \quad \hat{\sigma}_{\theta\theta}/Y = \left(2/\sqrt{3}\right)\cos(\varphi-\pi/3) \tag{5}$$

where φ is an auxiliary variable. In fact, Eq. (5) describes stress distributions in the plastic zone of the plate. Due to circular symmetry of the problem, $\hat{\sigma}_{rr} = \hat{\sigma}_{rr}(r)$, $\hat{\sigma}_{\theta\theta} = \hat{\sigma}_{\theta\theta}(r)$, and plane-stress assumption, $\hat{\sigma}_{zz} = 0$, there is only one non-trivial equilibrium equation

$$d\hat{\sigma}_{rr}/dr + \left(\hat{\sigma}_{rr}-\hat{\sigma}_{\theta\theta}\right)/r = 0 \tag{6}$$

which is valid both in elastic and plastic zones of the plate.

To conduct further analysis, the dimensionless parameters should be introduced: $\sigma_{rr} = \hat{\sigma}_{rr}/Y$, $\sigma_{\theta\theta} = \hat{\sigma}_{\theta\theta}/Y$, $p = \hat{p}/Y$; $\beta = r/b$, $\alpha = a/b$, $\gamma = c/b$, $\varepsilon_{rr} = \hat{\varepsilon}_{rr}E/Y$, $\varepsilon_{\theta\theta} = \hat{\varepsilon}_{\theta\theta}E/Y$, $u = \hat{u}E/(Yb)$.

In the inner plastic zone $\alpha\le\beta\le\gamma$, the solution of equilibrium Eq. (6) in parametric form (5) with the boundary condition (1) at $\beta=\alpha$ leads to an analytical expression defining the relation between the dimensionless radial coordinate β and auxiliary variable φ

$$\beta^2/\alpha^2 = \sin(\varphi_\alpha-\pi/6)\exp\left[\sqrt{3}(\varphi_\alpha-\varphi)\right]/\sin(\varphi-\pi/6) \tag{7}$$

where φ_a is the value of φ at $\beta=\alpha$ such that

$$\varphi_a = \arccos\left(-\sqrt{3}p/2\right) \tag{8}$$

From here, one may see that for a finite annular plate made of elastic-perfectly-plastic material, the value of maximum allowable pressure is $p = p_{\max} = 2/\sqrt{3}$.

The radius of the elastic–plastic boundary is determined by a simple formula

$$1/\gamma^2 = tg\left(\varphi_\gamma-\pi/6\right)/\sqrt{3} \tag{9}$$

where φ_γ is the value of ϕ at the elastic–plastic boundary γ which is expressed through the ϕ_a, Eq. (8), and a given size of the hole, α, Eq. (7), as follows:

$$\frac{1}{\alpha^2} = \frac{1}{\sqrt{3}}\exp\left[\sqrt{3}\left(\varphi_\alpha-\varphi_\gamma\right)\right]\frac{\sin(\varphi_\alpha-\pi/6)}{\cos\left(\varphi_\gamma-\pi/6\right)} \tag{10}$$

In the outer elastic zone $\gamma\le\beta\le1$, taking into account the condition of continuity of stresses at the elastic–plastic boundary, the stress-displacement solution is also defined analytically

$$\sigma_{rr}^E = \left(1-1/\beta^2\right)\cos\left(\varphi_\gamma-\pi/6\right), \quad \sigma_{\theta\theta}^E = \left(1+1/\beta^2\right)\cos\left(\varphi_\gamma-\pi/6\right) \tag{11}$$

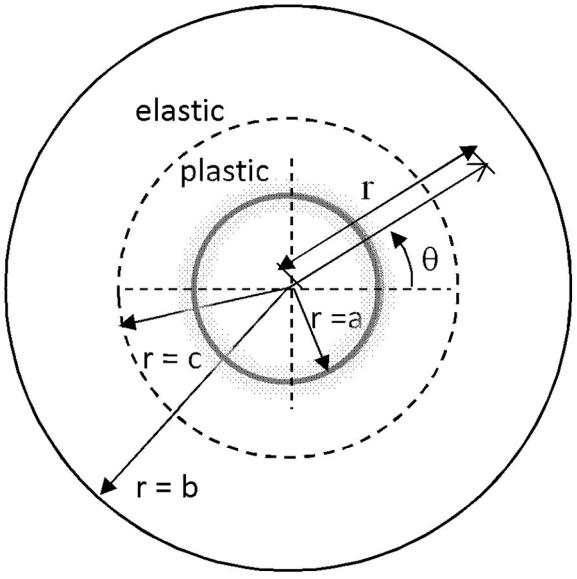

Fig. 1. Geometrical model of annular plate with elastic insert in cylindrical coordinate system.

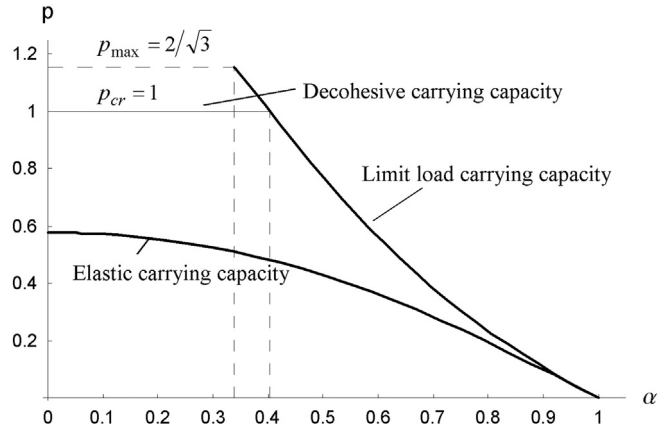

Fig. 2. Limit external loading curves.

$$u^E = [(1-\nu)\beta + (1+\nu)/\beta]\cos\left(\varphi_\gamma - \pi/6\right) \tag{12}$$

3. Kinematic analyses for fastener-hole structures in plastic zone

The total strain in the inner plastic zone of the plate is assumed to be the sum of elastic and plastic portions. The elastic portion is obtained from the Hooke's law (3) and stress distributions (5)

$$\begin{aligned}\varepsilon^e_{rr} &= \left[(2-\nu)\cos\varphi - \sqrt{3}\nu\sin\varphi\right]/\sqrt{3}, \quad \varepsilon^e_{\theta\theta} \\ &= \left[(1-2\nu)\cos\varphi + \sqrt{3}\sin\varphi\right]/\sqrt{3}\end{aligned} \tag{13}$$

The plastic portion is related to the proportionality relation offered by the Hencky–Ilyushin deformation theory

$$\varepsilon^p_{rr}/\varepsilon^p_{\theta\theta} = s_{rr}/s_{\theta\theta} \tag{14}$$

where ε^p_{rr} and $\varepsilon^p_{\theta\theta}$ are the radial and circumferential plastic portions of strains, respectively; s_{rr} and $s_{\theta\theta}$ are the radial and circumferential deviatoric components of stress tensor, respectively. So, Eq. (14) may be rewriting with the use of Eq. (5) in the form

$$\varepsilon^p_{rr} = \varepsilon^p_{\theta\theta}\left(\sqrt{3}\cos\varphi - \sin\varphi\right)/(2\sin\varphi) \tag{15}$$

Due to the general statement of the problem, in the plastic zone $\varepsilon^{Pz}_{rr} = \varepsilon^e_{rr} + \varepsilon^p_{rr} = \partial u/\partial\beta$ and $\varepsilon^{Pz}_{\theta\theta} = \varepsilon^e_{\theta\theta} + \varepsilon^p_{\theta\theta} = u/\beta$. Substituting Eqs. (13) and (15) into these equalities gives

$$\begin{aligned}\frac{\partial u}{\partial\beta} &= \frac{1}{\sqrt{3}}\left[(2-\nu)\cos\varphi - \sqrt{3}\nu\sin\varphi\right] + \varepsilon^p_{\theta\theta}\frac{\sqrt{3}\cos\varphi - \sin\varphi}{2\sin\varphi}, \\ \frac{u}{\beta} &= \frac{1}{\sqrt{3}}\left[(1-2\nu)\cos\varphi + \sqrt{3}\sin\varphi\right] + \varepsilon^p_{\theta\theta}\end{aligned} \tag{16}$$

Elimination of $\varepsilon^p_{\theta\theta}$ from the above Eq. (16) results in a differential equation for the radial displacement in the plastic zone

$$\frac{\partial u}{\partial\beta} - \frac{\sqrt{3}\cos\varphi - \sin\varphi}{2\sin\varphi}\frac{u}{\beta} = \frac{1-2\nu}{2\sqrt{3}\sin\varphi}\left(\sin 2\varphi - \sqrt{3}\cos 2\varphi\right) \tag{17}$$

which may be rewritten using ϕ-function (to be consistent with the main stress analysis) as an independent variable (instead of β)

$$\begin{aligned}&\frac{du}{d\phi} - \frac{\sin(\varphi-\pi/3)}{\sin(\varphi-\pi/6)}u \\ &\quad = -\frac{(1-2\nu)\alpha}{2\sqrt{3}}\frac{\left(\sin 2\varphi - \sqrt{3}\cos 2\varphi\right)}{[\sin(\varphi-\pi/6)]^{3/2}}\exp\left[\sqrt{3}/2(\varphi_\alpha - \varphi)\right]\sqrt{\sin(\varphi_\alpha - \pi/6)}\end{aligned} \tag{18}$$

Analytical solution of this equation has the following form:

$$u(\varphi) = \frac{\exp\left[\sqrt{3}/2(\varphi-\pi/6)\right]}{\sqrt{\sin(\varphi-\pi/6)}}\left(C + \int_{\varphi_\gamma}^{\varphi}\frac{\sqrt{\sin(\xi-\pi/6)}}{\exp\left[\sqrt{3}/2(\xi-\pi/6)\right]}\Phi_1(\xi)d\xi\right) \tag{19}$$

where Φ_1 is the right-hand side of Eq. (18) and C is a constant. Since the radial displacement u is a continuous function across the elastic–plastic boundary, the constant C in Eq. (19) is determined from the continuity condition for displacements

$$u\left(\varphi_\gamma\right) = u_\gamma \tag{20}$$

where $u_\gamma$is the value of u at the elastic–plastic boundary. Plugging $\beta = \gamma$ into Eq. (12) and using Eq. (9), it becomes

$$u_\gamma = \gamma\left[(1-\nu)\cos\left(\varphi_\gamma - \pi/6\right) + (1+\nu)\sin\left(\varphi_\gamma - \pi/6\right)/\sqrt{3}\right] \tag{21}$$

Finally, the radial displacement in the plastic zone is obtained by combining Eqs. (19)–(21).

$$\begin{aligned}u = \gamma&\left[(1-\nu)\cos\left(\varphi_\gamma - \pi/6\right) + \frac{1}{\sqrt{3}}(1+\nu)\sin\left(\varphi_\gamma - \pi/6\right)\right]\exp\left[\sqrt{3}/2\left(\varphi - \varphi_\gamma\right)\right] \\ &\sqrt{\frac{\sin\left(\varphi_\gamma - \pi/6\right)}{\sin(\varphi-\pi/6)}} + \frac{1-2\nu}{2\sqrt{3}}\alpha\sqrt{\frac{\sin(\varphi_\alpha - \pi/6)}{\sin(\varphi-\pi/6)}}\exp\left[\sqrt{3}/2(\varphi_\alpha + \varphi)\right]\int_{\varphi_\gamma}^{\varphi}\Phi_2(\xi)d\xi\end{aligned} \tag{22}$$

where $\Phi_2(\xi) = -\dfrac{\sin 2\xi - \sqrt{3}\cos 2\xi}{\sin(\xi - \pi/6)}\exp\left[-\sqrt{3}\xi\right]$

As soon as the displacement in the inner plastic zone is obtained, the total circumferential strain in this zone follows directly from Eq. (22), where u is divided by the dimensionless radius β. The elastic portion of circumferential strain is given by Eq. $(13)_2$ where function φ is

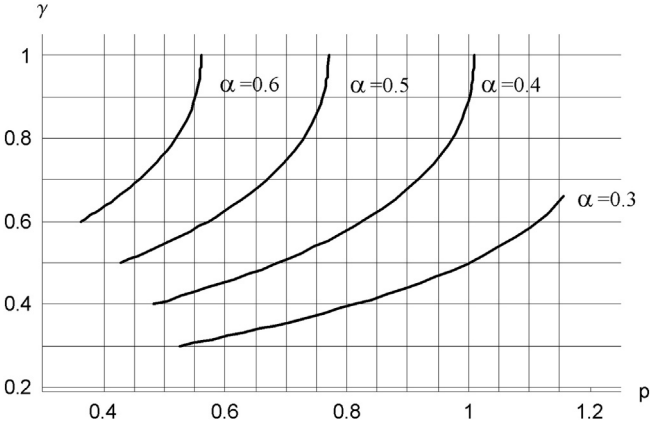

Fig. 3. Dependence of the elastic–plastic boundary on the pressure for various geometric ratios.

Table 1
Comparison of elastic–plastic boundary and circumferential strain obtained from analytical and finite element studies for various loading cases.

p/Y	0.65	0.75	0.85
c/a	1.066/1.065/1.010	1.164/1.165/1.150	1.273/1.265/1.250
$\varepsilon_{\theta\theta} = (u/a) \times 10^3$	3.42/3.24/3.42	4.17/4.17/4.11	5.20/5.19/5.00

replaced according to Eqs. (7)–(8) for specific values of pressure p and geometric parameter α (to provide distribution in coordinate β). Then, the plastic portion of circumferential strain is calculated as a difference between the total strain and the elastic portion. Knowing the plastic portion of circumferential strain, the corresponding plastic portion of radial strain is obtained from Eq. (15), and the elastic portion—from Eq. $(13)_1$, both with the help of Eqs (7)–(8). In the plastic zone, the coordinate β goes up to the elastic–plastic boundary γ which is defined for specific values of pressure p and geometric parameter α by means of Eqs (8), (10), and (9). In the outer elastic zone, the kinematic analysis is straightforward and based on Eqs (11)–(12) and (3) with parameter ϕ_γ derived from Eqs (8) and (10) for the same values of p and α.

4. Extension of kinematic analysis to interference-fit structures

In the case of double-shear riveted/bolted joints or, in broad sense, any elastic inclusion embedded with interference into elastic-perfectly-plastic plate, some adjustments to the analysis presented must be done. First of all, the stress–strain solution is not uncoupled any more due to the additional boundary condition on displacements at the bolt/plate connection. So, in fact, this type of problems is more elaborated, especially for the materials with different mechanical properties for the bolt and the plate.

As concerning elastic bolt, the stress-displacement solution is rather simple:

$$\hat{\sigma}_{rr}^{B} = \hat{\sigma}_{\theta\theta}^{B} = \frac{2}{\sqrt{3}}A, \quad \hat{u}^{B} = \frac{2}{\sqrt{3}}\frac{1}{E^{B}}\left[r(1-\nu^{B})A\right] \tag{23}$$

where A is a constant of integration; E^B and ν^B are modulus of elasticity and Poisson coefficient of the bolt, respectively. Applying boundary condition of continuity of radial stresses $\hat{\sigma}_{rr}^{B} - \hat{\sigma}_{rr}^{Plate} = 0$ at $r = a$ and taking into account that $\hat{\sigma}_{rr}^{Plate}(a) = -\hat{p}$, the constant A is found as $A = -\sqrt{3}\,\hat{p}/2$. So, Eq. (23) becomes

$$\hat{\sigma}_{rr}^{B} = \hat{\sigma}_{\theta\theta}^{B} = -\hat{p},\ \hat{u}^{B} = -r(1-\nu^{B})\hat{p}/E^{B}.$$

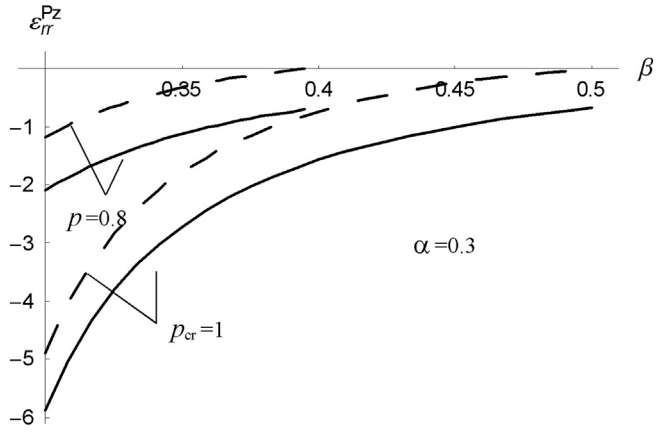

Fig. 4. Radial strain distributions in the plastic zone of the plate (dashed lines—plastic portions; solid lines—total values).

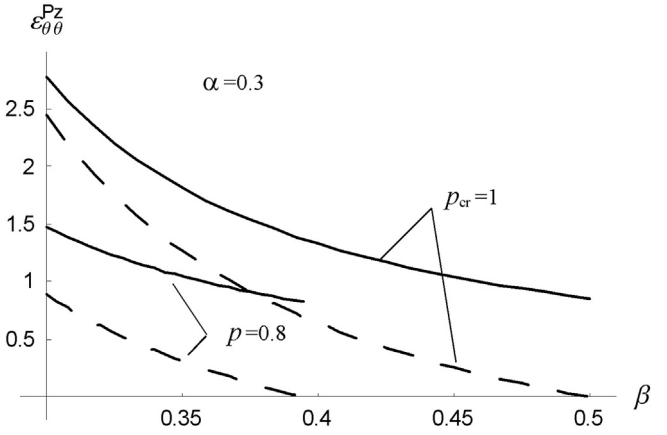

Fig. 5. Circumferential strain distributions in the plastic zone of the plate (dashed lines—plastic portions; solid lines—total values).

Introducing now dimensionless parameter $u^B = \hat{u}^B/b$ and keeping $p = \hat{p}/Y$, $\beta = r/b$, one gets the displacement field in the elastic bolt for further kinematic analysis

$$u^{B}(\beta) = -\beta(1-\nu^{B})pY/E^{B} \tag{24}$$

From here, the necessary additional boundary condition on displacements must be formulated at the bolt/plate interface

$$q + u^{B}(q) = \alpha + u(\alpha)Y/E \tag{25}$$

where $q = a^B/b$, a^B being the underformed radius of the bolt. Substitution of Eq. (24) at $\beta = q$ into Eq. (25) gives the value of initial radius of the bolt (before the embedment)

$$q = \frac{\alpha + (Y/E)u(\alpha)}{1-\left(Y/E^{B}\right)(1-\nu^{B})p} \tag{26}$$

where $u(\alpha)$ is defined from Eq. (22) at $\beta = \alpha$. So, the interference ratio for an elastic bolt is calculated as

$$Int_E = (q-\alpha)/\alpha \tag{27}$$

In the case of open fastener-holes, the analysis presented also permits an assessment of the residual permanent enlargement of the hole

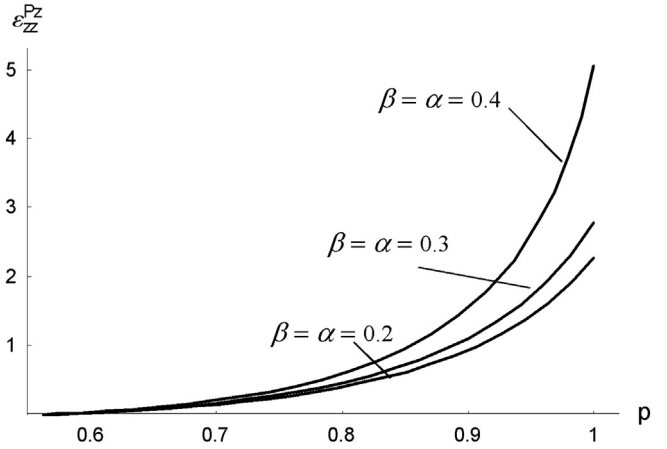

Fig. 6. Axial deformation at the bore of the hole as a function of pressure for various geometric ratios.

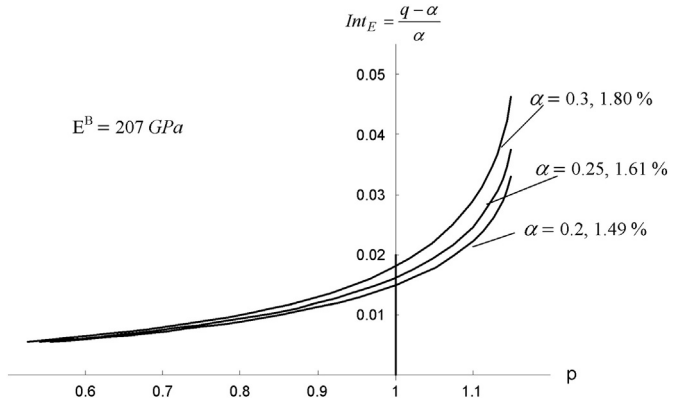

Fig. 7. Dependence of interference ratios on pressure for various geometric ratios in double-shear bolted joints.

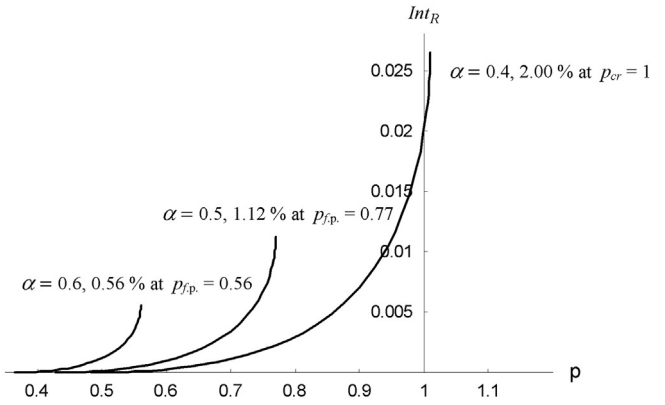

Fig. 9. Dependence of residual expansion ratios on pressure for various geometric ratios in general cold expansion processes.

(after the pressure p is removed) in terms of the residual expansion ratio

$$Int_R = \left(u(\alpha)/\alpha - u^{elastic}(\alpha)/\alpha\right)(Y/E) \tag{28}$$

where $u(\alpha)$ is defined from Eq. (22) at $\beta=\alpha$, and $u^{elastic}(\alpha)$ is the purely elastic solution for the radial displacement in an annular disk.

To this matter, the assessment of axial deformation at the fastener-hole location due to pressure may be important. Considering the most general case of compressible material, the sum of plastic and elastic portions of axial strain has been derived in the plastic zone of the plate

$$\varepsilon_{zz}^{Pz} = -\left(\sqrt{3}\cos\varphi + \sin\varphi\right)\left[\varepsilon_{\theta\theta}^{p}/(2\sin\varphi) + \nu\right] \tag{29}$$

where ϕ as a function of β, $\phi=\phi(\beta)$, is determined from Eqs. (7)–(8) for a specific pressure p and geometry α.

5. Discussion and conclusions

Numerical calculations are performed for an aluminum plate with the following mechanical properties: $Y=414\ MPa$, $E=69\ GPa$, $\nu=0.33$ [8] and an elastic inclusion (for example, steel bolt). It follows from the stress analysis that the maximum allowable pressure is $p=p_{\max}=2/\sqrt{3}$. This value corresponds to the hole size $\alpha=0.3376$ which implies that for $\alpha\le0.3376$, the plate never reaches its limit load carrying capacity (full plasticization), that is, some region of the plate near the outer radius will always be in the elastic state. For bolted structures, it means that the minimum distance between centers of bolts should be at least 2.96 times the bolt diameter ($b = 2.96a$). Hence, the analytical modeling of interference-fit structures presumes roughly $\alpha\le0.33$. Meanwhile, in general fastener-hole applications, geometrical ratio α goes up to 1, and for $\alpha>0.3376$, the plate reaches its limit load carrying capacity determined directly from the stress analysis for specific loads $p_{\max}\le2/\sqrt{3}$.

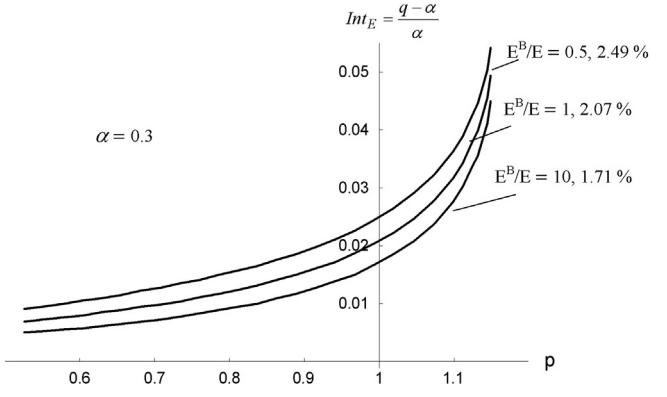

Fig. 8. Dependence of interference ratios on pressure for typical elastic moduli combinations in metal interference-fit structures.

However, to establish actual boundaries of external loading, a ductile failure criterion should be supplied based on the consideration of strains. One of the suitable criteria for interference-fit structures and elastic-perfectly-plastic material is so-called the decohesive carrying capacity criterion [29]. According to this criterion, the decohesion of the material may occur as a result of local infinite increase in radial strains, so a continuous deformation process terminates which automatically leads to the limit of serviceability of the structure. The review of papers dealing with problems of decohesive carrying capacity is given by Szuwalski [27] within elastic-perfectly-plastic material. For similar (to considered here) engineering problems, this criterion has been applied to a disk with rigid inclusion under various types of loading, namely, uniform tension at infinity [29], tension and in-plane torsion [30], tension and out-of-plane bending [31], and to a variable-thickness annular disk subjected to internal and external radial loading [32]. In most of these studies [29–31], at the moment of decohesion, radial strains increase infinitely at a disk/inclusion interface, and in [32]—at a particular location inside the disk.

In the present study, strain analysis shows that the tendency to infinity of radial strains from within the plastic zone also takes place along the connection of the plate material with the bolt. For this type of applications ($\alpha\le0.3376$), the deformation process is limited by the dimensionless critical pressure $p_{cr}=1$ (which is 13.4% less than $p_{\max}=2/\sqrt{3}$ obtained directly from the stress analysis). Apparently, this level of pressure corresponds to a stress condition such that the circumferential stress reaches zero at the bolt/plate interface. Indeed, due to Eq. (5), dimensionless stresses σ_{rr} and $\sigma_{\theta\theta}$ are functions of ϕ only, and their values at the bolt/plate interface are characterized by parameter ϕ_α which explicitly depends on pressure p, Eq.(8). So, for any α, critical stress condition $\sigma_{\theta\theta}=0$ at $\beta=\alpha$ occurs for $\phi_\alpha=5\pi/6$ and gives $p_{cr}=1$. Further increase of pressure leads to a separation of the bolt from the plate material. This behavior of plate/bolt connection is observed experimentally and has been studied from various engineering perspectives [33].

For general case of fastener-hole applications, the decohesive carrying capacity (occurring as well at $p_{cr}=1$) exists as a result of local infinite increase in radial strains at the border of the hole location. The value of α up to which this phenomenon persists is determined from Eqs. (7)–(8)

$$\alpha^2 = \sqrt{3}\exp\left[-\sqrt{3}(\varphi_\alpha-\pi/2)\right]/[2\sin(\varphi_\alpha-\pi/6)] \tag{30}$$

Plugging $\phi_\alpha = 5\pi/6$ into Eq. (30) gives $\alpha = 0.4037$. That is, within the interval $0.3377 \le \alpha \le 0.4037$, the c the limit load carrying capacity as a mechanism of failure in fastener-hole structures. Then, for $\alpha > 0.4037$, the ductile failure of interference-fit or cold expanded structures is dictated by the limit load carrying capacity mechanism. The curves bounded the elastic carrying capacity (when the material of the plate starts yielding), limit load carrying capacity, and decohesive carrying capacity are presented in Fig. 2.

The uncoupled stress solution, Eqs. (9)–(10), is also used to predict propagation of elastic–plastic boundary as a function of external loading. Besides the safe fastener-hole locations, the knowledge of the size of plastic zones in interference-fit structures is particularly important in a preliminary engineering design dealing with fatigue phenomenon. It was outlined by Jahed et al. [25] that for structures experiencing fatigue loads, the theories allowing for reliable residual stress calculations may be chosen on the basis of their capabilities to predict elastic–plastic zones since these zones are easier to measure experimentally than the residual stresses. The position of the elastic–plastic boundary as a function of pressure for various geometric ratios is shown in Fig.3. This plot may be used efficiently to relate the level of interference with the plastic zone propagation since the pressure and interference are mutually related parameters [8].

Since consideration of two separate zones, inner plastic and outer elastic, divided by an elastic–plastic boundary is a simplification of the real material behavior, the analytical solution proposed was compared with finite element results obtained by Pinho et al. [18] both for an elastic-perfectly-plastic material with $Y = 285$ *MPa*, $E = 71400$ *MPa*, $\nu = 0.3$ and real aluminum alloy Al 2024-T3 Alclad with the uniaxial stress–strain relation given (for $n = 8$) by

$$\varepsilon = \begin{cases} \sigma/E, & \sigma < Y \\ (Y/E)(\sigma/Y)^n, & \sigma \ge Y \end{cases}$$

The comparison is provided in Table 1 for various loading cases in the following sequence: present study/finite element study (elastic-perfectly-plastic model)/finite element study (real aluminum alloy). To simulate infinite plate considered in [18], the geometric ratio in the present study was chosen as $\alpha = 0.05$. From Table 1, it can be seen that an excellent agreement is achieved between the present analytical and finite element results.

Distributions of radial and circumferential strains in the plastic zone of the plate (marked by index "*Pz*" in the figures) for the critical (at the moment of decohesion) and some working pressures are presented, respectively, in Figs 4 and 5, where the dashed lines correspond to the plastic portion of strains and the solid lines correspond to the sum of elastic and plastic portions. Besides the tendency to infinity for radial strains, it can be clearly seen from both figures that it is very important to take into account the elastic portions of strains in plastic zone of the plate. Another conclusion is that there is a significant difference (up to 50% on the bolt/plate interface in absolute value) between plastic portion of radial strain and plastic portion of circumferential strain which shows the adequacy of the HMH yield criterion over the Tresca yield criterion (for which the equality of the absolute values of plastic radial and circumferential strains is assumed).

Other than that, the HMH yield criterion allows for an assessment of axial strains at the bore location in fastener-hole structures. It is shown in Fig. 6 that the axial strain increases rapidly as soon as the pressure reaches the critical value and is moderate for customary working loads. The axial strain for the critical pressure is comparable, in fact, with the circumferential one, and it is almost three times less for working pressures, so no appreciable thickening at the bore takes place during the deformation process. Being technically important by themselves, these results prove that the plane-stress model is more adequate than the plane-strain one (where it is presumed that $\varepsilon_{zz}^{Pz} = 0$), and is valid not only for fastener-holes but also for interference-fit structures. The effect of Poisson coefficient on the axial strain for a customary working pressure and various hole sizes may be observed directly from Eq. (29): this effect cannot be ignored and so the compressibility of the material both in the inner plastic and outer elastic zones should be taken into account.

Practical recommendations from the proposed strain analysis for engineering applications are mostly related to interference parameters. Fig. 7 shows predicted dependence of the interference ratio on the pressure up to $p_{\max} = 2/\sqrt{3}$ for several characteristic values of α in an aluminum plate with a steel bolt. The vertical axis line corresponds to the critical pressure $p_{cr} = 1$ for which decohesion (separation of the bolt from the surrounding plate) takes place. The interference ratio is higher for larger diameter bolts, and maximum safe values (corresponding to $p_{cr} = 1$) are marked (in percent) in the plot for each α. Besides the bolt size, the difference in elastic moduli for plate/bolt materials plays a significant role in the design of interference-fit structures. Some results for elastic bolts of varying stiffness are depicted in Fig. 8. These results coincide with [8] and indicate that the softer the bolt is, the higher the level of interference will be at a given pressure. The maximum safe values of the interference correspond to $p_{cr} = 1$ which are marked in the figure.

In general, while modeling fastener-hole applications within the elastic-perfectly-plastic material, two different failure mechanisms should be considered, namely, decohesive carrying capacity and limit load carrying capacity (depending on the ratio α). The dependence of residual expansion ratio (which also may be called as interference ratio with a removable mandrel) on pressure for several characteristic values of $\alpha$is presented in Fig. 9. The maximum residual expansion ratio (corresponding to $p_{cr} = 1$, decohesive carrying capacity criterion) is 2% which is attained for $\alpha = 0.4$. For larger holes, the plate reaches its fully plastic state (for a certain pressure $p_{f.p.}$), and limit load carrying capacity criterion then should be used to calculate residual expansion ratios.

References

[1] Hsu YC, Forman RG. Elastic–plastic analysis of an infinite sheet having a circular hole under pressure. Trans ASME J Appl Mech 1975;42:347–52.
[2] Lu WY, Hsu YC. Elastic–plastic analysis of a flat ring subject to internal pressure. Acta Mech 1977;27:155–72.
[3] Arora PR, Simha KRY. Analytical and experimental evaluation of coldworking process for strain hardening materials. Eng Fract Mech 1996;53(3):371–85.
[4] Bektas N, Altan G, Ergun E, Demirdal G. Elastic–plastic and residual stress analysis of an aluminum disc under internal pressures. J Eng Sci 2004;10(2):201–6.
[5] Bektas N. Elastic–plastic and residual stress analysis of a thermoplastic composite hollow disc under internal pressures. J Thermoplast Compos Mater 2005;18:363–75.
[6] Chakrabarty J. Theory of plasticity. 3rd ed. Elsevierdirect; 2006.
[7] Wanlin G. Elastic–plastic analysis of a finite sheet with a cold-worked hole. Eng Fract Mech 1993;46(3):465–72.
[8] Ball DL. Stress analysis of cold expanded fastener holes. Fatigue Fract Eng Mater Struct 1995;18(1):47–63.
[9] Gamer U, Lance RH. Elastisch-plastische Spannungen im Schrumpfsitz. Forsch Ing-Wes Bd 1982;48(6):192–8.
[10] Gamer U, Lance RH. Residual stress in shrink fits. Int J Mech Sci 1983;25(7):465–70.
[11] Gamer U. The elastic–plastic shrink fit with supercritical interference. Acta Mech 1986;61:1–14.
[12] Orcan Y, Gamer U. The shrink consisting of elastic hollow shaft and nonlinearly hardening elastic–plastic hub. Acta Mech 1990;81:97–108.
[13] Gamer U. A concise treatment of the shrink fit with elastic–plastic hub. Int J Solids Struct 1992;29(20):2463–9.
[14] Lundberg G. Die Festigkeit von Preβsitzen. Das Kugellager Bd 1944(1–2):1–11.
[15] Kollmann FG. Die Auslegung elastisch-plastisch beanspruchter Querpreβverbande. Forsch Ing-Wes Bd 1978;44(1):1–36.
[16] Akisanya AR, Khan FU, Deans WF, Wood P. Cold hydraulic expansion of oil well tubulars. Int J Press Vessel Pip 2011;88:465–72.
[17] Antoni N, Gaisne F. Analytical modelling for static stress analysis of pin-loaded lugs with bush fitting. Appl Math Modelling 2011;35:1–21.
[18] Pinho ST, Martins HB, Camanho PP, Santare MH, de Castro PMST. Residual stress field and reduction of stress intensity factors in cold-worked holes. Theor Appl Fract Mech 2005;44:168–77.
[19] Eraslan AN, Akis T. Yielding of two-layer shrink-fitted composite tubes subject to radial pressure. Forsch Ingenieurwes 2005;69:187–96.
[20] Lee EY, Lee YS, Yang QM, KIM JH, Cha KU, Hong SK. Autofrettage process analysis of a compound cylinder based on the elastic-perfectly plastic and strain hardening stress–strain curve. J Mech Sci Technol 2009;23:3153–60.
[21] Nadai A. Theory of flow and fracture of solids. New York: McGraw-Hill; 1950.

[22] Budiansky B. An exact solution to an elastic–plastic stress concentration problem. Prikl Mat Phys 1971;35(1):40–8.
[23] Zhang Y, Fitzpatrick ME, Edwards L. Analysis of the residual stress around a cold-expanded fastener hole in a finite plate. Strain 2005;41:59–70.
[24] Aleksandrova N. Engineering stress solutions for bolted and pressurized steel structures. Structures 2015;1:60–6.
[25] Jahed H, Lambert SB, Dubey RN. Variable material property method in the analysis of cold-worked fastener holes. J Strain Anal 2000;35(2):137–42.
[26] Wang Z, Zhang X. Predicting fatigue crack growth life for cold-worked holes based on existing closed-form residual stress models. Int J Fatigue 2003;25:1285–91.
[27] Szuwalski K. Decohesive carrying capacity in perfect and asymptotically perfect plasticity. Mech Teoretyczna Stosow 1990;28(1–2):243–54.
[28] Aleksandrova N. Influence of material compressibility on displacement solution for structural steel plate applications. J Eng 2014:1–7 [ID 413590].
[29] Szuwalski K, Zyczkowski M. On the phenomenon of decohesion in perfect plasticity. Int J Solids Struct 1973;7:85–98.
[30] Latas W, Zyczkowski M. Decohesive carrying capacity of a disk under tension and in-plane torsion. Int J Solids Struct 2000;37:1727–42.
[31] Szuwalski K. Decohesive carrying capacity of circular sandwich plate. J Theor Appl Mech 2000;38(2):403–15.
[32] Debski R, Zyczkowski M. On decohesive carrying capacity of variable-thickness annular perfectly plastics disks. ZAMM – Z Angew Math Mech 2000;82(10):655–69.
[33] HoangTD Herbelot C, Imad I. On failure mode analysis in a bolted single lap joint under tension-shearing. Eng Fail Anal 2012;24:9–25.